

Studies of the Antarctic sea ice edge and ice extent from satellite and ship observations

A.P. Worby^{a,*}, J.C. Comiso^b

^a*Australian Antarctic Division and Antarctic Climate and Ecosystems Cooperative Research Centre, University of Tasmania, Private Bag 80, Hobart, Tasmania 7001, Australia*

^b*NASA/Goddard Space Flight Center, Ice and Oceans Branch, Code 971, Greenbelt, MD 90771, USA*

Received 22 August 2003; received in revised form 7 May 2004; accepted 9 May 2004

Abstract

Passive microwave-derived ice edge locations in the Antarctic are assessed against in situ observations from ships between 1989 and 2000. During the growth season (March–October), the ship data agrees with satellite data very well, with r^2 values of 0.99 and 0.97 for the Bootstrap and Team algorithms, respectively. During the melt season (November–February), the agreement is not so good with the passive microwave ice edge typically 1–2° of latitude south of the observations. This is due to the low concentration and saturated nature of the ice, and the r^2 values for this period are 0.92 and 0.80 for the Bootstrap and Team algorithms, respectively. Sensitivity studies show that such an offset in the summer ice edge location can cause significant errors in trend studies of the extent of sea ice cover in the Southern Ocean. The passive microwave ice concentration at the ice edge observed by ship varies greatly, averaging 14% for the Team algorithm and 19% for the Bootstrap. Comparisons between passive microwave data and SAR, Landsat and OLS data during the ice growth season show that while small-scale details in ice edge location are lost, the passive microwave data generally provide good and consistent representation of the higher resolution imagery.

© 2004 Elsevier Inc. All rights reserved.

Keywords: Antarctic; Sea ice; Ice edge; Passive microwave; ASPECT

1. Introduction

The sea ice cover in both hemispheres is expected to respond sensitively to climate change, and evidence of this is suggested by a recent decline in Arctic sea ice extent (Bjørge et al., 1997; Cavalieri et al., 1997; Parkinson et al., 1999). In Antarctica, the passage of storm systems associated with the low pressure belt surrounding the sea ice zone (Jones & Simmonds, 1993) causes frequent changes in wind intensity, direction and temperature. This can cause daily shifts in ice edge location of up to 1° of latitude (Worby et al., 1998). The location of the ice edge is also highly seasonal and interannually variable, making the identification of long-term trends particularly difficult. The long-term ice edge location is influenced more by thermodynamic processes and may be influenced by changes in ocean

temperature and dynamics, and long-term changes in atmospheric circulation, on time scales of years to decades.

Satellite passive microwave (PM) data have been used to map ice extent on a daily basis in both the northern and southern hemispheres since 1972. The three decade-long time series provides a unique data set for investigating regional, seasonal and long-term changes in sea ice extent and has been used in innumerable scientific studies. A threshold in ice concentration of 15% has been used to define ice extent location in previous studies in order to eliminate unrealistic values caused by the influence in the near-open ocean region of wind and weather. Proper identification of the ice edge from PM data is important since the information is used across many scientific disciplines. For example, trends in sea ice extent may be linked to climate change, or to changes in oceanic and atmospheric circulation in the polar regions. Recent studies using PM data consistently show a decrease in Arctic ice extent over the past few decades (Bjørge et al., 1997; Cavalieri et al., 1997; Parkinson et al., 1999) while the results of similar studies in the Antarctic are ambiguous (Bjørge et al., 1997; Cavalieri et al., 1997; Comiso, 2003;

* Corresponding author. Tel.: +61-3-6226-2985; fax: +61-3-6226-7650.

E-mail address: A.Worby@utas.edu.au (A.P. Worby).

Zwally et al., 2002). PM data have also been used to identify trends and variability in the ice edge location over shorter time periods and specific regions of the pack (e.g., Ackley & Keliher, 1976; Jacobs & Comiso, 1993), and are important in studies of marine biology because the ice edge is a key location for phytoplankton blooms (e.g., Sullivan et al., 1988). The mean ice edge location derived from PM data is also used extensively as a validation tool in modelling studies (e.g. Stössel et al., 1990) and for comparison with palaeoclimate data derived from geological proxy measures such as faunal census and stable isotope analyses (Schweitzer, 1995).

Some proxy records suggest that the Antarctic sea ice extent was significantly further north in the past. Sediment and ice-rafted-debris interpretation of deep sea cores suggest that during the last glacial maximum an ice cover persisted for 6–7 months of the year as far north as 56.4°S at longitude 145.3°E (Armand & Leventer, 2003). This is 6.3° further north than the mean contemporary maximum (derived from SMMR and SSM/I data) at the same longitude. The maximum ice extent at this location during the passive microwave record is 59.8°S. Also, using more recent but still historical data from whaling ships, de la Mare (1997) reported a southward shift of the summer ice edge (October–April) by 2.8° of latitude between the mid-1950s and early 1970s. Curran et al. (2003) suggest a similar decrease in summer sea ice extent of 22% since the 1950s, for the region 80–140°E, based on MSA records from the Law Dome ice core. They show a positive relationship between MSA, the biogenic sulphur compound produced from marine algae, with passive microwave sea ice extent records since 1973, and suggest that summer biological activity (MSA production) is enhanced in years when the maximum September extent is greatest. Parkinson (1990) compared historical data from early explorers of the 19th century with contemporary data to examine possible changes in ice edge location. Some significant differences between the data sets were found, showing the historical ice edge both north and south of the 1973–1976 passive microwave ice edge; however, overall Parkinson found no compelling evidence of a substantial change. In contrast, Wu et al. (1999) compared the same historical data with passive microwave data from 1988 to 1995 and showed a mean decrease in ice extent of 1.17° latitude from Cook's 1777 data, and 1.03° latitude from Bellingshausen's 1831 data. They also simulated a decrease in mean sea ice extent for the same period using a coupled global climate model, although this was less than their observed decrease from the historical observations to the 1988–1995 passive microwave record.

The question raised in long-term ice extent variability studies is how consistently the ice edge location is determined by historical and contemporary data? Satellite microwave data provide the most spatially and temporally consistent measurement for sea ice, but we have seen that results even from the same data set (but using different algorithms) provide inconsistent trends, especially in the Antarctic (Bjørge et al., 1997; Cavalieri et al., 1997). It is

also not known what the sensor really sees as the ice edge (usually defined as 15% ice concentration) especially since the emissivity of sea ice is highly variable in the region. In this paper we aim to better understand the information from PM data through comparative analysis with other satellite data and contemporary ship observations of the sea ice edge. We first compare the PM data with in situ data from ships to evaluate the variability in ice edge location on a smaller spatial scale. Through this study, we can then evaluate how reliable historical and contemporary in situ observations are in terms of defining the ice edge location and how consistent such data are with the satellite-observed ice edge. We then compare examples of PM-derived ice edge locations using the Bootstrap algorithm with coincident SAR, Landsat and OLS data to assess the consistency in ice edge location between satellite sensors. Issues affecting ice edge retrieval such as instrument resolution, daylight requirements and weather effects are discussed.

2. Ship observations of the ice edge

In situ observations of the Antarctic sea ice edge have been compiled from voyages which were part of the Australian and US Antarctic programs between 1989 and 2000. This is a subset of the Antarctic Sea Ice Processes and Climate (ASPeCt) data archive that has been compiled from sea ice records kept by numerous national Antarctic programs between 1980 and the present. Trained sea ice observers were onboard each cruise and the data have been quality controlled and compiled into a standard format. The data archive is currently housed at the Australian Antarctic Data Centre (<http://www.aad.gov.au>) but will soon be accessible via a dedicated website. For this paper, a total of 36 ice edge crossings have been used. Only voyages which clearly transect the ice edge while travelling in a north–south direction were used. This excludes a considerable amount of data from voyages that intersected the ice edge while travelling in an east–west direction, because on those voyages ice could have been present north of the recorded ice edge. For the purpose of this analysis, we define the ice edge observed by ship as the northernmost occurrence of sea ice of at least 10% concentration. This includes bands of ice that may be detached from the main body of the pack by substantial stretches of open water, hence the concentration on a 25-km grid scale could be less than 10%. Observations of changes in ice conditions from the ship as a function of latitude are especially useful in establishing the true character of the ice margin that can then be compared with the satellite data. They are also particularly useful for establishing standards when comparing data from different sources (e.g., visible, infrared and microwave data). For example, instead of using the arbitrary value of 15%, such data could provide the basis for the determination of an optimal ice concentration value that should be used for ice extent analysis. Also, the ship data could provide the means to

find out which features of the ice edges are uniquely identified by the different sensors.

The ship observations have all been recorded using a standard protocol specified by the Antarctic Sea Ice Processes and Climate (ASPeCt) program within the Scientific Committee on Antarctic Research (SCAR). The protocol is described by Worby and Allison (1999) and Worby (1999). Total ice concentration is estimated from the ship's bridge within a 1-km radius of the ship to the nearest 10%, and the partial concentrations of the dominant three ice types are recorded to the nearest 10%. Ice type is recorded using World Meteorological Organisation classifications and the thickness, floe size, topography and snow cover characteristics of each type are also recorded. Since ice concentration is measured to the nearest 10%, there is a rounding error of up to 5%. Observer error is difficult to quantify; however, tests of coincident observations by different observers rarely differ by more than 10% in total concentration. We therefore estimate the error in total and partial concentrations to be 10%. Errors in the partial concentrations are also estimated at 10%. Ice type classification errors should be minimal given that the observers are trained in sea ice nomenclature.

Ice conditions at the ice edge are highly variable, especially due to seasonal changes that affect sea ice growth and decay and thus the surface properties of the ice. During the growth season, between March and October, it is not uncommon to find pancake ice at the ice edge; however, this is not necessarily the norm due to frequent changes in wind direction and temperature. Periods of rapid expansion can occur that result in bands of ice and shuga, while northerly winds may compact the ice so that the edge is a well-defined line of quite consolidated ice (Worby et al., 1998). When this occurs the ice concentration can go from 0% to 100% within one satellite pixel. Massom et al. (1997) and Worby et al. (1998) have shown that even in winter, air temperatures within the pack ice zone can rise to 0 °C, particularly near the ice edge. This could result in surface melt and a change in surface properties, and therefore microwave properties, of the ice and snow cover.

In the melt season, the ice edge tends to comprise lower concentrations of decaying floes with varying amounts of brash ice between them, often saturated by waves and melted snow. Fig. 1(a)–(c) shows examples of different ice conditions near the ice edge that would most likely not be detected by the passive microwave instrument. Fig. 1(a) is an example of the bands of ice that are sometimes present at the ice edge and might be observed at any time of year. These bands can be quite high concentration and comprise mostly brash ice and small saturated and decaying floes. Bands like this can be several hundred metres to a kilometre across and are usually separated by stretches of open water up to several kilometres wide. Alternating bands of ice and open water have been observed over more than a degree of latitude as discussed in Section 4. Fig. 1(b) is an example of decaying ice floes that can be found north of the main body of the pack ice, usually broken up, wave-washed and in low

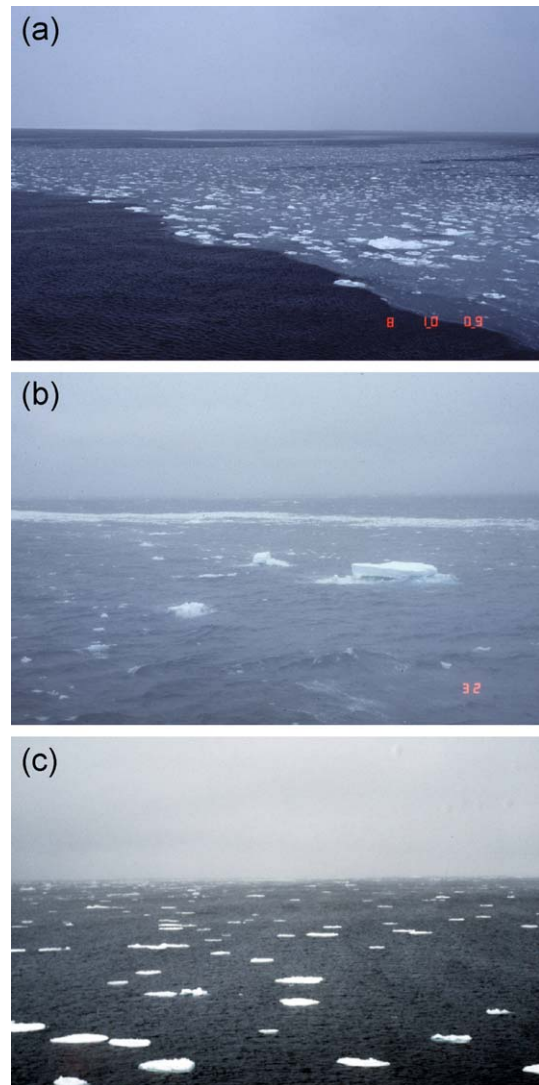


Fig. 1. Photographic images of different ice conditions at the ice edge that would most likely not be seen in satellite passive microwave data. (a) Bands of mostly saturated ice of quite high concentration, usually separated by stretches of open water; (b) old decaying floes and brash ice; and (c) small disperse floes of about 1/10 ice concentration.

concentrations. These conditions are typical of late spring and summer. Fig. 1(c) is another example of diffuse ice conditions of approximately 1/10 concentration. Each of these examples represents ice conditions that an observer on a ship would define as the ice edge. It is also highly likely that such conditions would have been recorded by early explorers and whaling vessels as the ice edge, even if they were able or willing to continue further south. The overcast weather conditions shown in each image are also typical of the ice edge region.

3. Satellite observations

Passive microwave data have been used to assess trends in sea ice extent on different spatial and temporal scales.

Ackley and Keliher (1976) used the first two full years of ESMR data to evaluate the variability of the location of sea ice extent and spatial distribution of ice concentration between 1973 and 1974. They showed significant regional differences in ice extent between the two years but commented that this did not reflect a change in total extent due to compensating changes in different regions. Similarly, a significant decrease in summer ice extent in the Bellingshausen Sea from 1998 to 2001, reported by Comiso et al. (1997), was coincident with large increases in the Ross Sea for the same period (Zwally et al., 2002). Earlier studies by Gloersen and Campbell (1991) and Zwally et al. (1991) looked for trends in Antarctic sea ice extent for the periods 1978–1987 and 1973–1988, respectively. Neither found any significant trends over the longer term.

A more recent study using PM data combined corrected SSMR and SSM/I data for the period 1978–1996 using the NASA Team algorithm, and shows an increase of 1.3% per decade in the mean annual ice extent in Antarctica (Cavalieri et al., 1997; Zwally et al., 2002). Using an updated data set to cover 22 years of passive microwave data from 1978 to 2000, Comiso (2003) shows an increase of only 0.3% per decade using the Bootstrap algorithm, while Bjørge et al. (1997) show a decrease of 1.1% over the period from 1978 to 1995 using the NORSEX algorithm. The differences in trend analyses arise in part because each algorithm effectively defines the ice edge differently, and this highlights the problems associated with accurately deriving sea ice parameters from satellite PM data. In contrast, all three studies show a decrease in Arctic ice extent over the same period, as does Parkinson et al. (1999). The asymmetry in ice extent trends between the polar regions observed in two of the studies is consistent with a modelled response to a carbon dioxide-induced global warming (e.g., Manabe et al., 1992).

The advantage of passive microwave satellite data is the synoptic and continuous day/night coverage of the polar surface in almost all weather conditions. A disadvantage is the relatively coarse resolution of about 25×25 km. This problem is minimized through the use of an algorithm that calculates the percentage of ice within the satellite footprint (Comiso et al., 1997).

Color-coded ice concentration maps from SSM/I data derived from the Bootstrap and Team algorithms are shown in Fig. 2(a) and (b), respectively. The images show the same general characteristics of the circumpolar ice edge and ice extent; however, there are significant differences in the interior of the pack (Comiso et al., 1997). Detailed comparisons of ice concentrations from the two algorithms in conjunction with OLS, AVHRR, and Landsat data were reported in Comiso and Steffen (2001), who showed that in areas where differences between the Team and Bootstrap algorithms is high, Landsat data are in better agreement with the Bootstrap values. In this paper, we are mainly interested in the ice edge location and the consistency of locating the 15% ice edge and surrounding regions. Although the ice

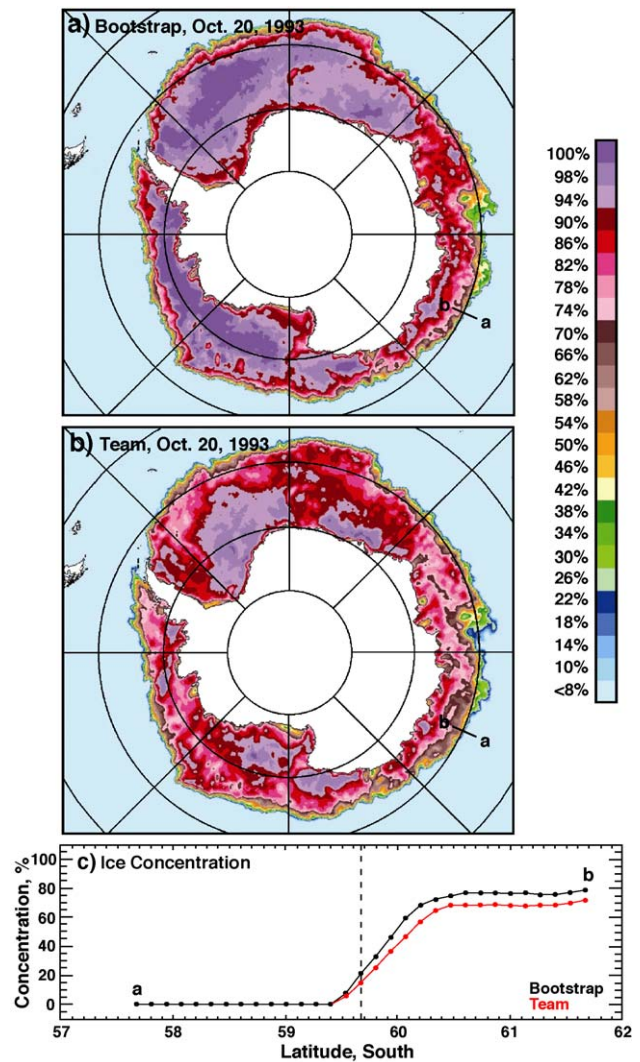


Fig. 2. (a) Antarctic ice concentration map on October 20, 1993 using the Bootstrap algorithm; (b) Antarctic ice concentration map on October 20, 1993 using the Team algorithm; and (c) ice concentration as a function of latitude for both Bootstrap and Team algorithms along the transect line indicated in (a) and (b).

concentration technique is a factor, the ice edge location at the 10–15% level is mainly controlled by the masking technique which is designed to eliminate unrealistic retrievals of ice concentrations in the open ocean such as those associated with adverse wind and weather conditions (Bootstrap: Comiso, 1995; Team: Gloersen et al., 1992).

To illustrate the changes in the ice cover across the ice edge, a transect across the ice edge near 100°E is shown in Fig. 2(a) and (b) and labeled 'a' and 'b' at the end points. The corresponding ice concentration values along these transects for both Bootstrap and Team algorithms are shown in Fig. 2(c). The latter shows very similar distributions for the ice concentrations from both algorithms; however, the Bootstrap reveals significantly higher values in the interior pack than the Team. This is consistent with findings reported in Comiso et al. (1997) and is discussed further

in Section 4.1. The transect a–b represents the track of the icebreaker RSV Aurora Australis on 20 October 1993, and the vertical dash line in Fig. 2(c) is the location of the ice edge as observed from the ship. The consistency of the location and characteristics of the circumpolar ice margin is encouraging, indicating that the ice edge location can be identified consistently even with different techniques. The lack of spatial resolution; however, becomes a weakness in terms of finding the exact location of the ice edge from PM data. With SSM/I data, for example, the ice edge cannot be defined any better than the 25×25 km grid. The ship data provide better resolution but basically only in one dimension, hence there is a mismatch in the spatial coverage of the observations. While the ship data provide what can be the true location of the ice edge at one particular spot, this location may not reflect the ice cover averaged over a 25×25 km grid.

Other satellite sensors have been used for monitoring the ice cover with mixed success. Among these is the Synthetic Aperture Radar (SAR) which also provide day/night and all weather coverage but the spatial and temporal coverages are very limited, especially in the Antarctic. The data, however, provide very detailed coverage of the surface, when available, with the resolution being typically 30×30 m. High resolution data are also available in the visible channel, as can be obtained from Landsat, SPOT, and similar sensors. These systems are good for ice studies and easiest to interpret, but surface data are available only during daytime and cloud-free conditions, and like SAR, the spatial coverage is very limited. Other visible sensors provide better spatial coverage at intermediate resolution, such as AVHRR (1.1 km resolution) and OLS (2.5 km resolution). These sensors provide global/orbital coverage but again are restricted to daytime/cloud-free conditions. Scatterometers like NSCAT and QUICKSCAT also provide good spatial coverage, but at lower resolution (25–50 km resolution) and with a relatively short record length compared to the passive microwave data. Algorithms for ice parameters are still being developed for scatterometer data (Kwok et al., 1999).

4. Comparison of passive microwave data with ship observations

In this study, the location of the PM ice edge is taken to be the mid-point of the northernmost SSM/I pixel with ice concentration $\geq 10\%$, thus introducing an error of ± 12.5 km. We use the daily averaged SSM/I products instead of single overpasses to reduce the bias from side lobe effects. Sensitivity studies have shown that this has little effect on the slope in ice concentration across the ice edge (Comiso & Zwally, 1984). We then interpolate between points to the position of the ship observation which defines the ice edge. Our aim is to determine whether or not the sea ice edge observed by ship is also that observed by the PM data, and whether or not this is seasonally consistent. Since we are

only concerned with the location of the ice edge, we do not attempt to further resolve the spatial differences between the two data sets.

4.1. March–October (ice growth season)

Comparison of the ship and passive microwave ice edge data shows a range of results. During the ice growth season, between March and October, the agreement is very good. Typically, the ice edge is advancing during these months when the air temperature is cold enough to keep the ice concentration fairly high. As a consequence, the ice edge is usually quite compact. Ship observations at this time of year show the transition from the northernmost occurrence of ice to consolidated pack ice usually occurs over just 10–20 nautical miles (18–36 km), or 1–2 SSM/I pixels. Fig. 3(a) shows an example from 21 July 1998 along 147.2°E . The ship data show a rapid increase in ice concentration from 63.7°S to 64.3°S which is also reflected in the PM data. There is good agreement in the location of the ice edge. The ship data show ice concentration values from 2 to 10 tenths, then an area of open water around 64.5°S . The PM data show less extreme variability in concentration because of smoothing effects caused by the larger footprint of the data. Also, at least 2/10 of the ice is identified as brash, which is usually saturated with seawater and will not be well represented in the SSM/I concentrations. The example shown in

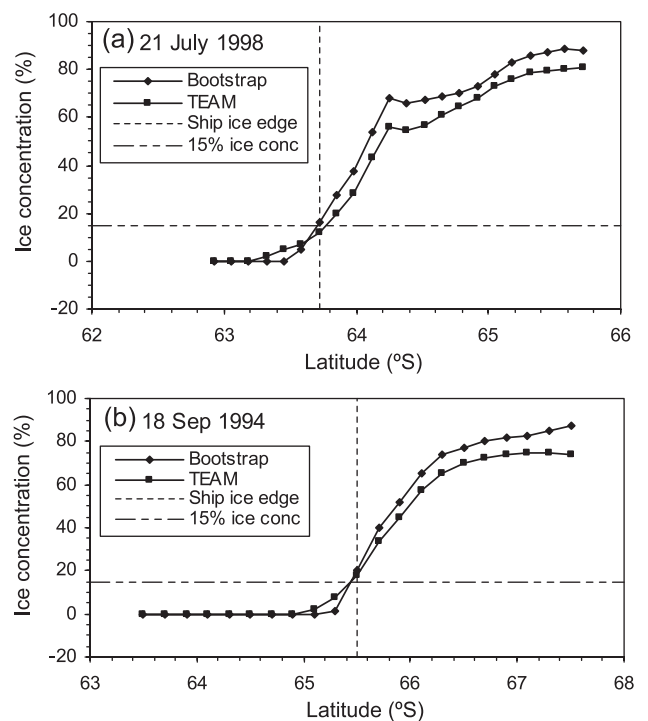


Fig. 3. Bootstrap and Team ice concentrations for (a) July 21, 1998 along 147.2°E , and (b) September 18, 1994 along 107.8°W . In both figures, the latitude of the ice edge observed by ship is shown as a vertical dashed line. The 15% passive microwave concentration threshold is shown as a horizontal dot-dash line.

Fig. 3(b) is from the other side of the continent on 18 September 1994 at 107.8°W. The ice here was all first year 0.3–0.8 m thick, predominantly level or with 10% surface ridging up to 0.5 m high. Again, there is good agreement in ice edge locations between observations and the two SSM/I algorithms—because at this time of year the PM data are effective at determining the location of the ice edge because of the large contrast in the emissivity of ice and water at some frequency channels. Fig. 3(a) and (b) also shows the Bootstrap has ice concentrations around 10% higher than the Team inside the main body of the pack ice. This is a typical pattern during the ice growth season, because the Team uses polarization ratios which are sensitive to layering in the snow, and the snow/ice interface (Matzler et al., 1984).

Fig. 4(a) and (b) shows the relationship between the ship observations and the SSM/I Bootstrap and Team algorithms,

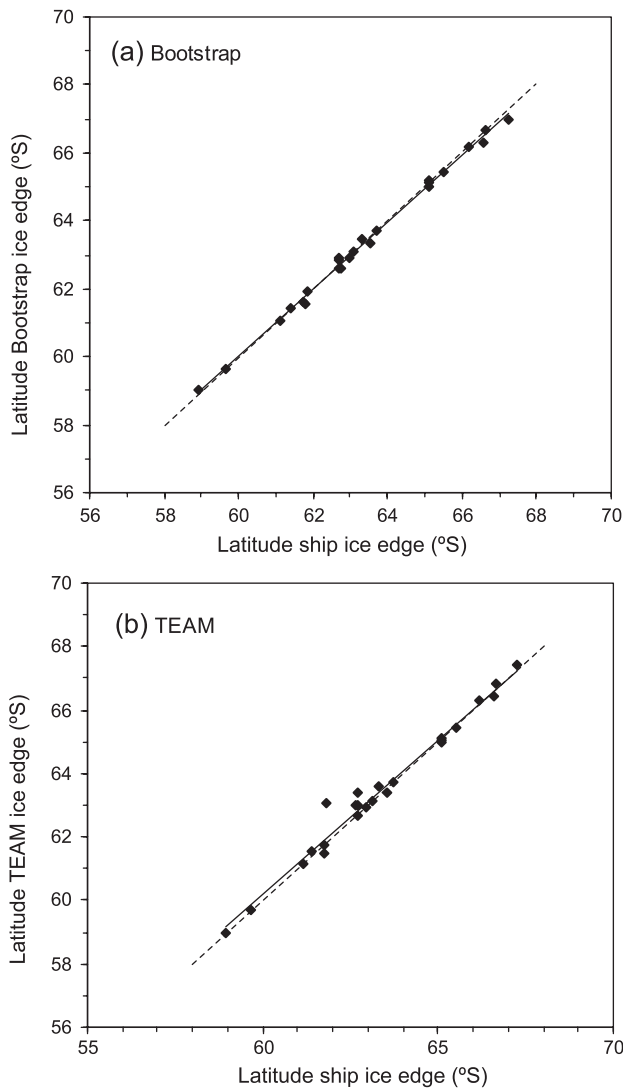


Fig. 4. Latitude of the ice edge observed from ship versus the SSM/I ice edge for data in the period March–October for (a) Bootstrap and (b) Team algorithms. The solid black line shows the linear trend. The dashed line represents the 1:1 relationship.

Table 1
Ship location information and coincident SSM/I data at the 36 ice edge data points discussed in the text

Date	Ship-observed ice edge		SSM/I ice edge latitude ^a		SSM/I ice concentration ^b	
	Latitude (S)	Longitude ^c	Team	Bootstrap	Team	Bootstrap
29-Mar-93	65.12	139.83	65.1	65.1	16	15
30-Mar-93	65.1	141.27	65	65.21	1	22
21-Apr-95	65.12	147.57	65.02	64.99	27	22
7-May-98	66.65	179.95	66.8	66.7	11	7
9-May-95	66.2	179.73	66.3	66.2	16	9
21-Jul-98	63.72	147.18	63.74	63.7	16	13
22-Jul-99	61.77	142.88	61.5	61.54	30	25
26-Jul-98	62.7	143.25	63.01	62.62	18	1
29-Jul-95	61.75	139.85	61.76	61.6	33	15
3-Aug-95	62.7	179.87	63.38	62.88	0	0
26-Aug-95	63.1	139.83	63.15	63.09	16	11
27-Aug-95	67.23	-110.1	67.45	66.98	28	7
31-Aug-99	62.72	146.58	62.64	62.6	28	22
8-Sep-94	58.95	149.98	58.98	59.01	4	12
12-Sep-95	63.55	-76.75	63.4	63.33	43	31
18-Sep-94	65.5	-107.8	65.44	65.44	21	18
24-Sep-93	66.58	-109.9	66.41	66.31	46	30
2-Oct-97	61.83	114.5	63.08	61.95	4	0
14-Oct-94	63.32	-172.25	63.57	63.46	0	0
16-Oct-90	61.13	115.32	61.17	61.03	25	12
17-Oct-91	62.67	137.87	62.98	62.82	4	1
20-Oct-93	59.67	114.32	59.69	59.61	21	15
20-Oct-91	62.95	137.39	62.93	62.89	24	16
27-Oct-94	61.42	111.37	61.54	61.42	15	10
5-Nov-91	60.02	106.03	61.45	61.26	0	0
5-Nov-98	59.78	113.38	61.05	60.71	0	0
10-Nov-90	60.17	83.62	61.1	60.52	0	0
19-Nov-91	59.42	85.81	61.78	61.02	0	0
23-Nov-94	61.78	100.8	62	61.89	2	1
23-Nov-00	63.47	110.97	63.98	63.91	0	0
2-Dec-89	61.7	81.72	63.18	62.84	0	0
2-Dec-99	64	153.75	65.28	65.28	0	0
18-Dec-98	61.75	71.95	65	63.35	0	0
12-Jan-00	63.4	88.2	63.4	63.45	15	8
1-Feb-00	65.2	110.7	66.4	65.43	1	9
7-Feb-00	65.16	109.31	65.43	65.22	6	9

^a This is the latitude of the passive microwave ice edge along the same longitude as the ship-observed ice edge.

^b This is the passive microwave ice concentration at the ship-observed ice edge.

^c Positive values are °E, negative values are °W.

respectively, for the 36 ice edge crossings presented in Table 1. During the growth season, there is excellent agreement between the data sets, with r^2 values of 0.99 for the Bootstrap and 0.97 for the Team. The difference between the ship and PM observations is calculated using the exact location of the ship observation and the centre of the SSM/I pixel. From these calculations, the mean Bootstrap ice edge is $0.04 \pm 0.13^\circ$ latitude (within 1 pixel) north of the ship observations while the mean Team ice edge is $0.11 \pm 0.31^\circ$ latitude (within 1–2 pixels) south of the ship observations. The 1:1 relationship is shown in Fig. 4(a) and (b) as a dashed line. The mean concentration values at the observed ice edge during the March–October period are 19% for the

Bootstrap and 14% for Team, although the scatter is highly variable as shown in Table 1.

At any time of the year southerly winds may cause the ice to diverge and bands of ice of varying concentration separated by stretches of open water may be found at the ice edge. Fig. 5(a) is from a transect across the ice edge on 26 July 1998 and shows an example of an ice edge comprised of bands in mid winter. Between 62.7° and 63.8°S bands of variable ice concentration were present, with ship observations showing consolidated ice >80% south of 63.8°S. Such conditions were observed at a number of ice edge crossings, and on each occasion the Bootstrap algorithm shows higher concentration ice that is more consistent with the ship observations than the Team. There are two examples in the ship's data record (August 3, 1995 and October 2, 1997) when bands of ice and open water extend more than 1° of latitude south of the observed ice edge (using our definition of the northernmost ice of at least 10% concentration) during the growth season. On these occasions, the two algorithms differed in their ice edge location by more than 150 km (6 pixels), with the Bootstrap in much better agreement with the ship observations. The October 2, 1997 example is shown in Fig. 5(b) and includes the ice concentration observed from the ship south of the ice edge. This highlights how some abnormalities at the ice edge can

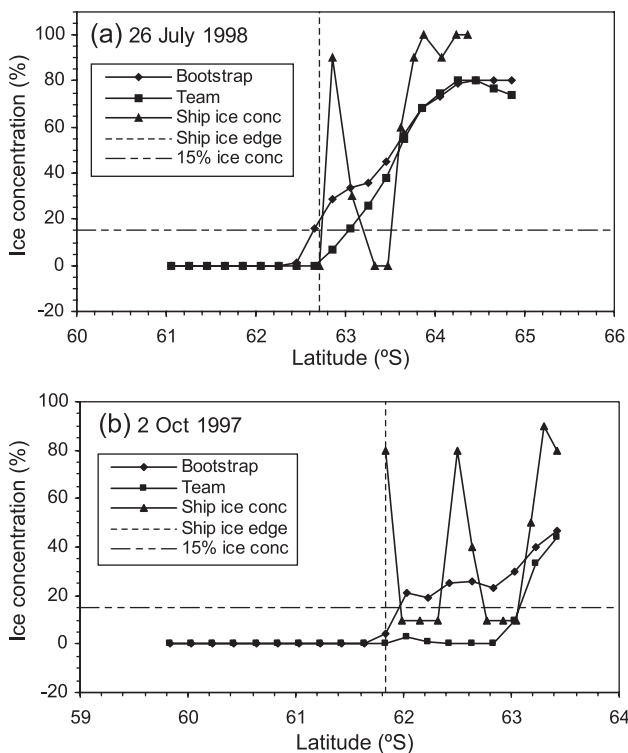


Fig. 5. Bootstrap, Team and ship-observed ice concentrations for (a) 26 July 1998 along 143.25°E and (b) 2 October 1997 along 114.5°E. On both occasions, bands of ice were present at the ice edge. In both figures, the latitude of the ice edge observed by ship is shown as a vertical dashed line. The 15% passive microwave concentration threshold is shown as a horizontal dot-dash line.

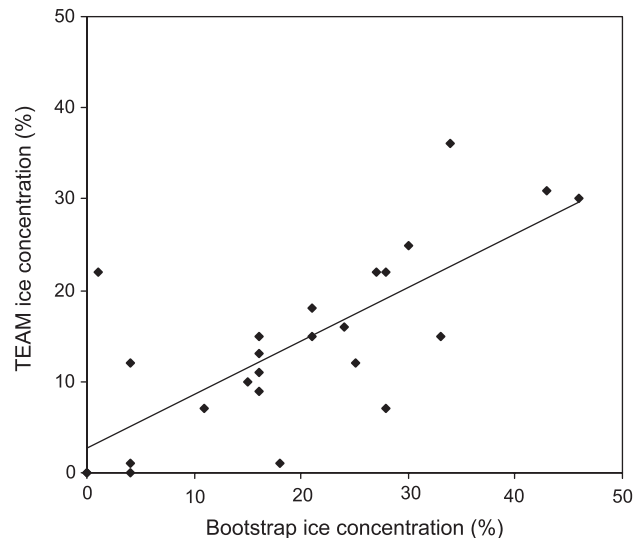


Fig. 6. Scatter plot showing Bootstrap versus Team ice concentration values at the latitude of the ice edge observed by ship. Data are for the March–October period between 1989 and 2000. The solid black line shows the linear trend.

provide questionable results from satellite data. Fig. 6 shows that the ice edge concentrations for the Team and Bootstrap algorithms are poorly correlated, with $r^2 = 0.55$. These range between -21% and $+21\%$ with the Bootstrap higher than the Team at all but three points. This is consistent with the findings of Comiso and Steffan (2001) that showed generally higher concentrations for the Bootstrap algorithm south of the ice edge in the pack ice zone.

4.2. November–February (ice decay season)

November through February are months of net ice decay in all sectors of the Antarctic pack ice (Gloersen et al., 1992). During these months, the pack ice decays rapidly both at the ice edge and from within the pack, resulting in reduced extent and concentration. Divergence of floes enhances melt due to increased absorption of solar radiation by the ocean, which increases the lateral and bottom melt of floes. The floes also tend to be saturated as a result of snow melt and wave action. The bands of ice common at the ice edge can be quite high concentration, say 5–10 tenths, and could therefore easily have been considered by early explorers or whalers as a “hard” ice edge. However, because the ice is saturated, and often comprises a high percentage of brash, the passive microwave signature of the surface may be very close to that of seawater. Additionally, the bands may be less than 10% concentration when averaged over a 25×25 km pixel, and consequently neither algorithm agrees well with ship observations at this time of year.

Typically, bands of ice and open water extend 1–2° latitude south of the ice edge in November and December, and this is reflected in the poor agreement between data sets. Fig. 7 shows three examples of such conditions. In

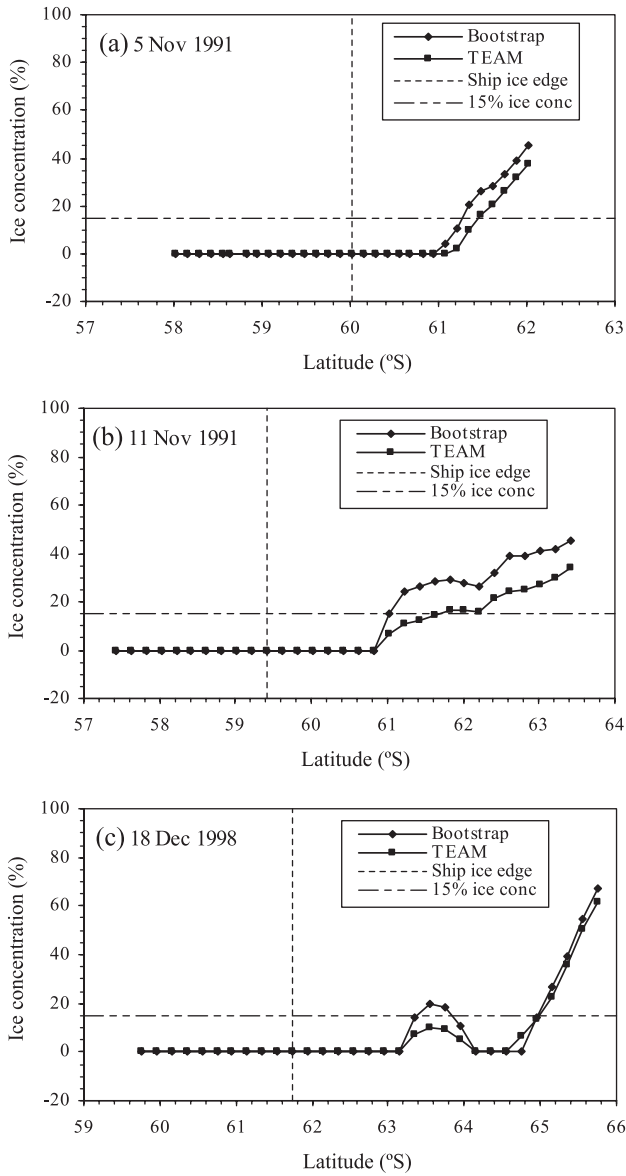


Fig. 7. Bootstrap and Team ice concentrations for (a) 5 November 1991 along 106.03°E, (b) 11 November 1991 along 80.84°E, and (c) 18 December 1998 along 71.95°E. In all figures, the location of the ice edge observed by ship is shown by a vertical dashed line. The 15% passive microwave concentration threshold is shown as a horizontal dot-dash line.

Fig. 7(a), the first bands of ice were observed by ship at 60.02°S, 106.03°E. These were up to 3/10 concentration, with as much as 1/10 thick multiyear floes. However, the bands were very localized and therefore below the concentration threshold when averaged over the area of an SSM/I pixel. South of the ice edge bands there was a 90-km stretch of open water before more consolidated ice was encountered at 61°S, which was observed by the PM instrument. In Fig. 7(b), the ice edge observed by ship at 59.42°S, 80.84°E was very diffuse, with repeated bands of ice and open water over several degrees of latitude. These first occurred more than a degree north of where the PM first detects ice, and the concentration of the pack ice was

1–2 tenths concentration over this region. South of 61°S the concentration remained fairly low, mostly between 2 and 4 tenths, and the Team algorithm shows considerably lower concentration values than the Bootstrap in this region. This is consistent with the discussion of Fig. 5. Fig. 7(c) is a more extreme example which shows the PM response to sea ice approximately 1.5° south of the observed ice edge, which comprised 1–2 tenths brash approximately 0.5 m thick between 61.75°S and 63°S along 71.95°E. Although both algorithms clearly respond to the more consolidated ice south of 63°S, the Team concentration does not reach the 15% threshold. It is not until the heavier ice in Prydz Bay is reached south of 64.8°S that the Team algorithm reaches the 15% threshold, which is more than 3° south of the ice edge observed by ship.

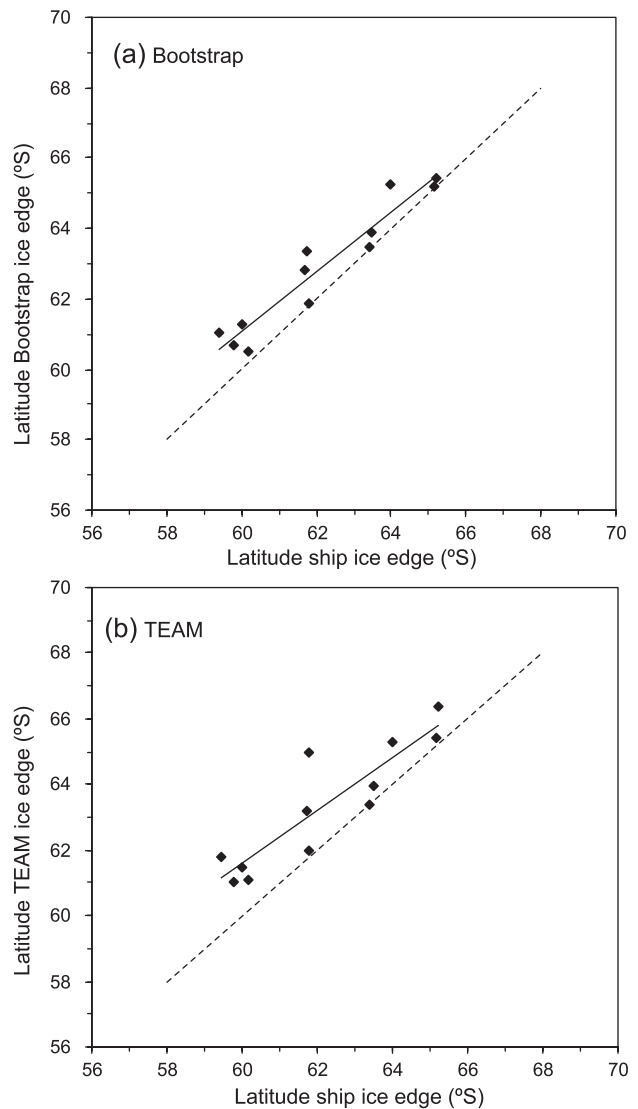


Fig. 8. Latitude of the ice edge observed from ship versus the SSM/I ice edge for data in the period November–February for (a) Bootstrap and (b) Team algorithms. The solid black line shows the linear trend. The dashed line represents the 1:1 relationship.

Fig. 8(a) and (b) shows the relationship between the ship observations during the November–February period, and the Bootstrap and Team algorithms, respectively. The r^2 values are 0.92 for the Bootstrap and 0.80 for the Team. The difference between the ship and SSM/I ice edge locations is calculated using the exact location from the ship data and the midpoint of the SSM/I pixel. On average the Bootstrap ice edge is $0.75 \pm 0.61^\circ$ latitude (3 pixels) south of the observed edge during the melt season, while the Team ice edge is $1.18 \pm 0.93^\circ$ latitude (5 pixels) south of the observed ice edge. None of the melt season SSM/I ice edges are north of the ship observations, and consequently the melt season data do not fall along the 1:1 line (shown by the dashed line in Fig. 8) in the same way as the growth season data. There is a distinct offset, converging toward a 1:1 relationship near

the coast, as a result of the SSM/I algorithms failing to see the ice furthest north. The mean ice concentration at the observed ice edge for both algorithms is 0%.

5. Effects of seasonal bias

A sensitivity study was carried out to assess the effect of a summer bias on the long-term trend in Antarctic sea ice extent. The results are shown in Table 2 and are based on a 1-, 2-, 3- or 4-pixel increase to the SSM/I (Bootstrap) ice edge during the ice decay season, i.e., November through February. The effect on the trend was relatively insignificant, as might be expected given that the PM data applies a consistent threshold to determine the ice extent location.

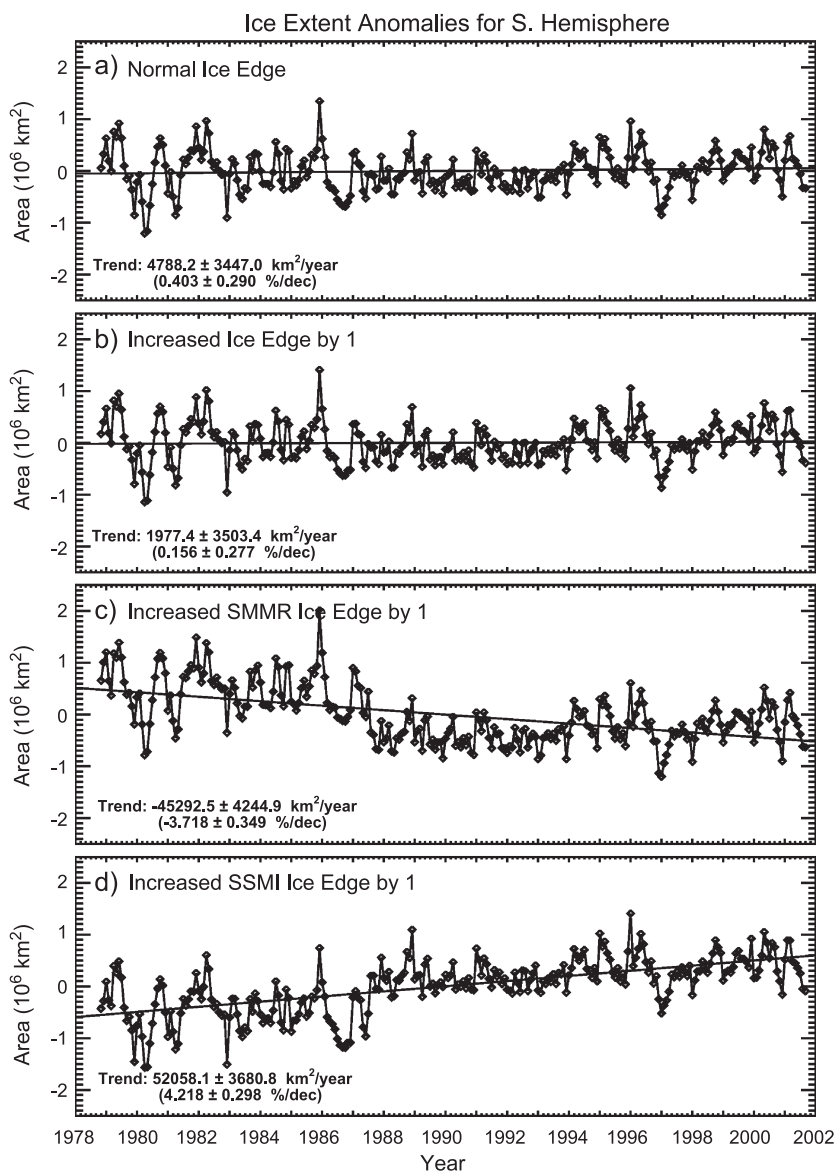


Fig. 9. (a) Observed ice edge and trend analysis for the passive microwave record from 1978 to 2002 using the Bootstrap algorithm; (b) ice edge and trend analysis when a 1-pixel increase in ice extent is applied to each month of the record; (c) ice edge and trend analysis when a 1-pixel increase is applied only to the SMMR record; (d) ice edge and trend analysis when a 1-pixel increase is applied only to the SSM/I record.

Table 2

Results of a sensitivity study showing the change in long-term ice extent trend for a 1-, 2-, 3- or 4-pixel increase in ice extent during the decay season (November through February)

No. of pixel increase	Trend in sea ice extent (% per year)
1	0.371
2	0.438
3	0.479
4	0.501

There is however a small increase in trend as the bias is increased, reaching +0.5% per decade for a 4 pixel (approximately 1° latitude) increase. This is a more significant trend than reported by Comiso (2003), suggesting that a more northerly summer ice edge may have some effect on the long-term ice extent trend.

Fig. 9 presents results from a second sensitivity study which applied a 1 pixel bias to the entire data set and also to the SSM/I and SSMR data sets separately. One pixel is chosen as the smallest unit of error in the measurements. Fig. 9(a) shows the observed ice edge for the passive microwave record from 1978 to 2002 using the Bootstrap algorithm published by Comiso (2003). The reported trend for this data is a slightly significant +0.3% per decade increase in sea ice extent. Fig. 9(b) shows that when a 1-pixel increase in ice extent is applied to each month of the record there is an insignificant effect on the long-term ice extent trend; however, Fig. 9(c) and (d) shows the large change in ice extent trend when a 1 pixel bias is applied to the SSMR and SSM/I data separately. A trend of -3.7% per decade is observed when the bias is applied to the SSMR data but not to the SSM/I data (Fig. 9(c)), and a +4.2% per decade trend is observed when the bias is applied to the SSM/I data but not to the SSMR data (Fig. 9(d)). This highlights the sensitivity of the long-term ice extent trend to small changes in ice edge location, and therefore the importance of having substantial overlap (at least a year) between sensors to ensure consistency of data used in long-term trend studies. This is an especially important consideration when the sensors do not have the same spatial resolution, as is the case between the SSMR and SSM/I sensors. A bias between these sensors of about 1 pixel at the ice edge is possible.

6. Large-scale comparison

To gain insight into the possible differences between PM data and other satellite data, we compare a number of coincident images at the Antarctic sea ice edge. As described above, PM data provide the only global, daily data set of ice edge location, but have the coarsest resolution (25 km), and therefore the greatest potential for spatial errors. Here we compare SSM/I Bootstrap data with RADARSAT/SAR (28 m resolution), LandSat 7 Thematic

Mapper (TM) (30 m resolution) and OLS (560 m resolution) imagery to assess the large-scale agreement between these data products.

Fig. 10(a) shows an ice concentration map using the Bootstrap algorithm on May 6, 1998. The rectangular region outlined in this image is coincident with the 30 × 30 m resolution RADARSAT/SAR image from the same date shown in Fig. 10(b). Some low concentration features are labeled a, b and c in both images as a reference guide in the comparative analysis and to indicate that the two sensors are sensitive to the same open water features within the pack. The 15% and 30% ice concentration contours determined from the SSM/I data are shown on the SAR image. Detailed

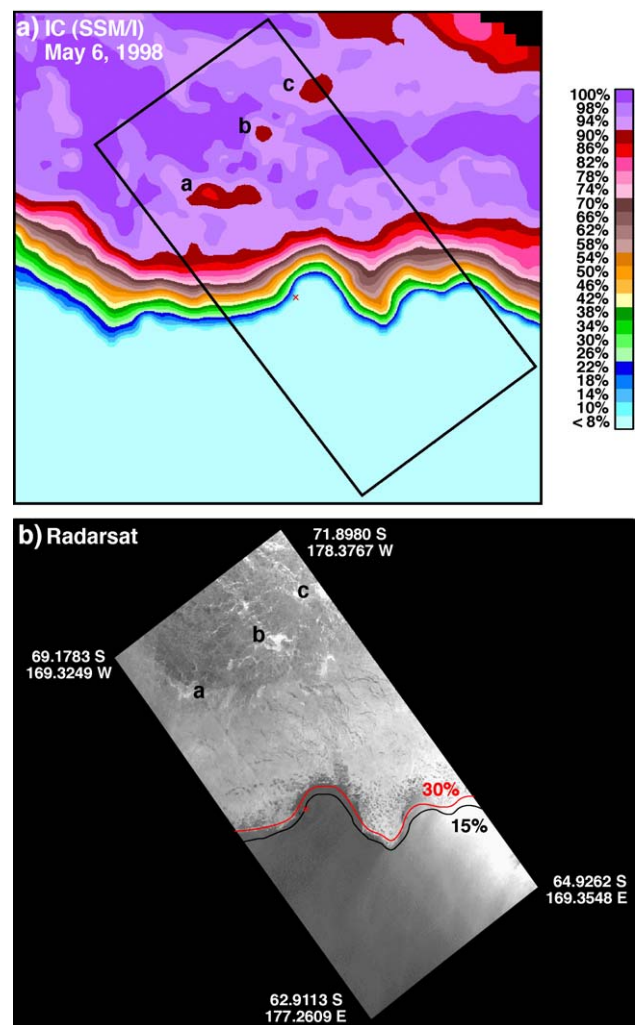


Fig. 10. (a) Antarctic ice concentration map on May 6, 1998 using the Bootstrap algorithm; (b) SAR/RADARSAT image on May 6, 1998 in the location of the black rectangle in (a). The ice concentration contours shown on the SAR image in (b) are the 15% and 30% contours from the SSM/I image in (a). RADARSAT image files are R113059721P4U008 and R113059721P4U009 taken on May 6, 1998 at 08:22:13 and 08:23:14 UTC, respectively. The ship crossing of the ice edge (marked with a red × on the images) occurred at 66.65°S, 179.95°E on May 7 at 2300 UTC. North is at the top of the page.

examination of these two lines indicate that, as expected, the SAR data provide spatial details of the ice margin that are not apparent from the SSM/I data. However, it is obvious that the SSM/I lines provide a good reproduction of the ice edge contour on a large scale. To improve the presentation of contours a smoothing is done on the PM image by interpolating 9 subgrids from each of the 25×25 km grids; however, the quantitative analysis is done using the original grid. It is also apparent that the 15% contour is sometimes in an area where the SAR data do not indicate the presence of an ice cover. Despite its high resolution, SAR data could express such ambiguity in ice identification at the ice margin if the ice cover is flooded or if the ocean surface is covered by grease ice, small pancakes or thin nilas

(Grenfell et al., 1992). It is, however, most encouraging that the overall shape of the ice edge is very similar for both SAR and SSM/I data, and this supports the results from Section 4 that during the growth season, the PM data define the ice edge quite reliably. Furthermore, it is encouraging that the 30% ice edge contour closely follows the line of the 15% contour. This indicates that the ice threshold used in the algorithms provide credible ice edge distributions because the 30% contour is less dependent on the ice threshold than the 15% contour. The location of the ship at the time it reached the ice edge the following day (2300 UTC on May 7) is indicated by a red \times in both figures. The ship data indicate an air temperature of -2.4 °C and wind speed of 10 m s^{-1} from 270°T , so it is consistent that the ice edge

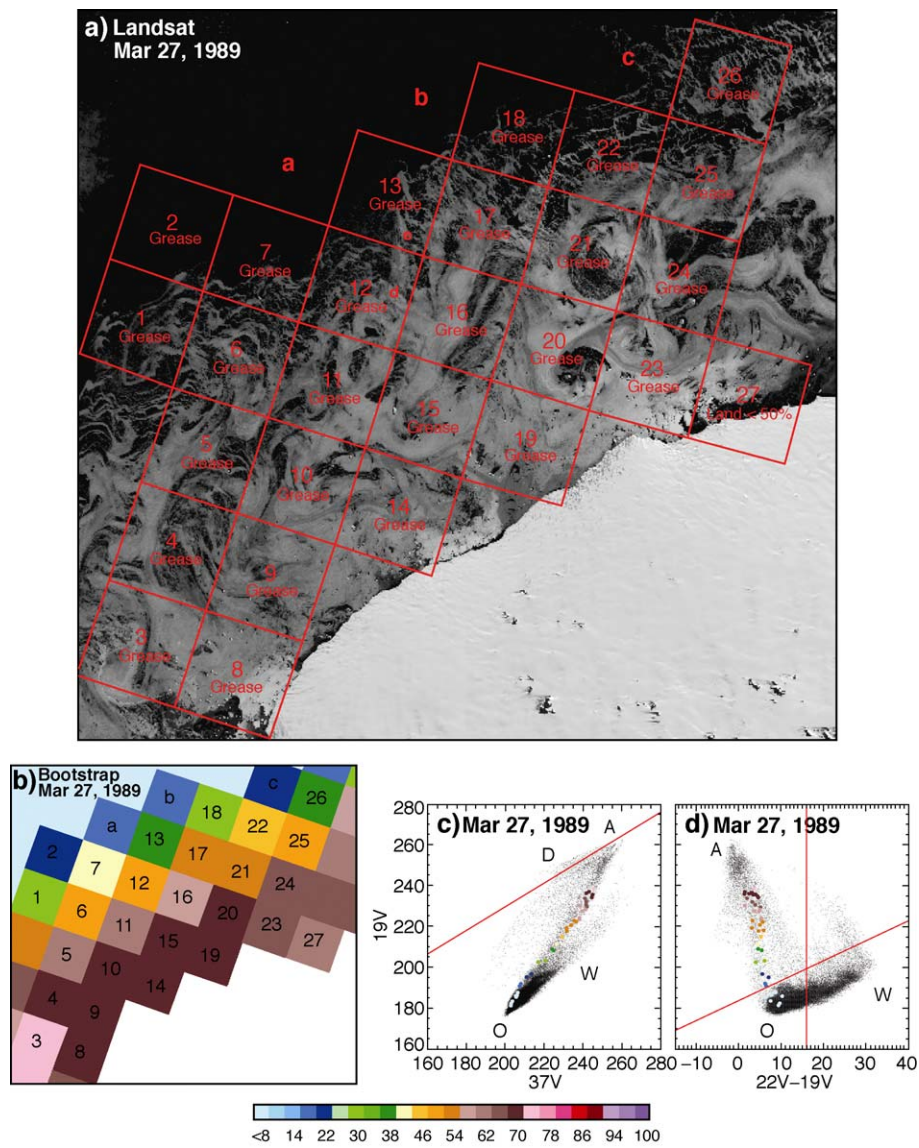


Fig. 11. (a) Landsat image in the Cosmonaut Sea of the Antarctic region on March 27, 1989 with rectangular grids corresponding to colocated SSM/I grid; (b) SSM/I ice concentration data co-registered with the Landsat image; (c) scatter plot of 19V versus 37V with ice edge pixels indicated in color; (d) scatter plot of 19V versus $(22V - 19V)$ with ice edge pixels indicated in color. The color scale shows ice concentration in percent.

shown in the satellite data is slightly to the east of the ship location on May 7. Unfortunately, coincident SAR data (within ± 1 day) could not be found for any other ice edge crossings used in this study.

When SSM/I data are compared with high resolution Landsat (visible) data, similar results are apparent. Fig. 11(a) is a Landsat TM image at the Cosmonaut Sea ($\sim 50^\circ\text{E}$) on March 27, 1989 with a resolution of 30 m. The corresponding ice concentrations from the Bootstrap algorithm (at approximately the same scale) are shown in Fig. 11(b). The two images are co-registered with the rectangular grid in the Landsat image labeled the same way as the corresponding SSM/I pixels. The boxes labeled a and b are clearly shown by the Landsat image to be ice-free while the SSM/I data indicates 15% ice concentration. This happened during an early growth period and it is likely that there are small pancakes (a few cm in diameter) such as those described by Wadhams et al. (1987) in regions that are identified by Landsat as ice-free. This is because the reflectivity of this type of ice cover is about the same as that of open water (Allison et al., 1993). Fig. 11(c) and (d) shows scatter plots of 19V versus 37V and 19V versus 22V–19V, respectively (units of GHz). The data from ice edge pixels, including a and b, are color-coded in the scatter plots and indicate the location of these data points with respect to the open water tie point. As discussed in Comiso et al. (1997), the cluster along the line AD in Fig. 11(c) corresponds to a consolidated ice cover while the cluster of data along OW correspond to open water data points. The cluster OW is shown to be more distinct and easier to separate when plotted as in Fig. 11(d). The 15% threshold for ice concentration is indicated by a horizontal red line above O and W in Fig. 11(d) and it is apparent that the ice edge pixels are close to this threshold. Data points below the near horizontal red line are identified as open water, as are data points to the right of the vertical red line, and together these define the ocean mask. The data points corresponding to the pixels a and b are not within the ocean mask as described, suggesting that they are likely surfaces covered, or partly covered, by ice. It may not be possible to discriminate these from open water in the Landsat image.

On a larger scale, Fig. 12(a) shows OLS data from the Amundsen Sea region on September 1, 1995 while the corresponding SSM/I ice concentration map derived using the Bootstrap algorithm is shown in Fig. 12(b). The two images are not perfectly registered but for geographical reference, the black rectangles in the images delineate the same geographic locations. The problem with cloud cover in the visible data is apparent in Fig. 12(a), especially in the open ocean and parts of the marginal ice zone. However, there is enough cloud-free area along the ice edge that enables qualitative comparisons of the two images. The 15% and 30% ice concentration contours shown on the OLS image are transposed from the SSM/I image for comparison. Once again, while the passive microwave data do not show the good spatial detail available in the higher resolution OLS

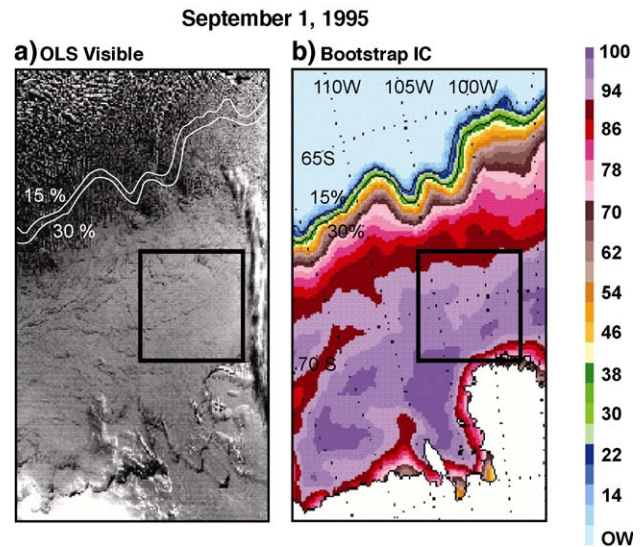


Fig. 12. (a) OLS image on September 1, 1995 in the Amundsen Sea; (b) ice concentration map from SSM/I data using the Bootstrap algorithm on September 1, 1995 in the same area. The color scale shows ice concentration in percent (OW = open water).

data, the contours are, in general, very similar and the former provide consistent and reliable information. As in the comparison with Landsat, the SSM/I contours are again to the north of the ice edge observed in the OLS image. In addition to the presence of small pancakes that are not detectable by the OLS sensor, there could also be cloud-shadowing effects that decrease the albedo of the ice surface.

7. Discussion and conclusions

The location of the sea ice edge is closely linked to climatic conditions, and accurately defining it is fundamentally important if reported trends in ice extent are to be meaningful. Studies of palaeo ice extent generally agree that during the last glacial maximum (LGM), the ice extent was significantly north of its present location (Armand & Leventer, 2003; Crosta et al., 1998); however, there are differing reports of ice extent variability over the past 50–200 years (Curran et al., 2003; de la Mare, 1997; Parkinson, 1990). There is even inconsistency between the trends reported from the passive microwave data, available since 1978, depending which algorithm is used (Bjørge et al., 1997; Cavalieri et al., 1997; Comiso, 2003).

The results of comparisons between passive microwave data and ship observations show a clear seasonal effect on the reliability of the PM-derived ice edge. During the growth season, when the pack ice is consolidated, the ice edge can clearly be defined and the SSM/I ice concentration threshold has been shown to agree exceptionally well with ship observations. Overall, results from the Bootstrap algorithm are in slightly better agreement with the ship observations than the Team, although both show a high

correlation with the in situ data. During the ice decay season, however, the location of the ice edge determined from both SSM/I algorithms is in poor agreement with the observed ice edge, due to lower ice concentration and warmer, saturated ice. Again, the Bootstrap algorithm is in better agreement with the observations than the Team, and this may influence the choice of algorithm used for some applications. However, neither algorithm can claim to accurately represent the true ice edge at this time of year, and the application of a summer correction to PM data or improvements in the algorithms for this time period should be further investigated.

Sensitivity studies show that a uniform summer bias has little effect on trends derived solely from the PM data; however, large discrepancies occur when a bias is applied to either the SMMR or SSM/I time series, or when the satellite data are compared with historical data from another source. Typically, the observed ice edge is in a range of 1–2° latitude north of the PM ice edge during the summer season. This bias clearly has the potential to influence the accuracy of long-term ice edge studies making use of ship data, whether historical or contemporary, when compared with SSM/I ice edges based on the 15% concentration threshold. [de la Mare \(1997\)](#) showed a summer decrease in sea ice extent of 2.8° latitude based on a comparison of whaling records from the mid-1950s with satellite passive microwave data starting in the 1970s. The proxy measure of sea ice extent from the whaling records is based on the whale catch regions, routinely reported to be at the edge of the Antarctic pack ice. Our results suggest that during the summer months the passive microwave ice edge derived from the Team algorithm (which was used by [de la Mare](#)) is an average of 1.18° latitude south of the ship observed ice edge. [Ackley et al. \(2003\)](#) showed that when this bias is taken into account, the southward shift in ice edge location reported by [de la Mare](#) falls within the observed variability of ice edge location. The results of this paper are slightly revised from [Ackley et al.](#) but report a similar shift in ice edge location. Similarly, historical log book entries by [Cook and Bellingshausen](#) reported ice between 2° and 10° north of the early 1970s SSM/I data in the summer months ([Parkinson, 1990](#)). On most occasions, these could unambiguously be identified as isolated fields of ice, or part of an ice tongue, laying well north of the rest of the pack ice at the same longitude, because large areas of open water were reported further south.

[Armand and Leventer \(2003\)](#) report that palaeo sea ice distribution data allow scientists to develop a better understanding of the relationship between climate change and sea ice. The palaeo record is typically compared with the modern day record derived using the PM Team algorithm ([Schweitzer, 1995](#)) that shows maximum extent during the LGM to be between 5° and 8° latitude north of its present location ([Crosta et al., 1998](#)). [Crosta et al. \(1998\)](#) also discuss the importance of determining both the summer and winter sea ice extent during the LGM in

order to better understand Southern Ocean palaeoceanography and palaeoclimatology. For summer reconstructions in particular, determining the net change from modern day conditions will need to carefully consider both the differences in algorithm performance and seasonal variability reported here.

The comparisons of PM data with higher resolution satellite data show that while the small-scale detail in ice edge location is lost, the PM data do provide a representative ice edge location that is consistent with the other sensors. While there may be local wind and weather effects that cause ambiguity on occasions, such as the anomaly shown in the SAR data, the contours quite faithfully follow the ice edge shown in the higher resolution data in the examples we have shown during the ice growth season. For long-term assessments of ice extent, the passive microwave data are an invaluable tool. They provide the only global, daily coverage of sea ice extent in both hemispheres and thus provide valuable insights into the climatic response of sea ice. Improvements in future PM data acquisitions could be made by ensuring at least a 12-month overlap between successive sensors. This would allow for improved data sets through advancing technology and the ability to correct earlier data to ensure a continuous and consistent data record. Further improvements necessary for accurately and consistently identifying the ice edge include a good definition of an ice edge, especially considering that there are many types of ice edges, and an ice concentration algorithm capable of supporting it.

List of acronyms and terms

AVHRR	Advanced Very High Resolution Radiometer
Bootstrap	Comiso algorithm for interpreting passive microwave data
NASA	National Aeronautics and Space Administration
NORSEX	Norwegian Remote Sensing Experiment
NSCAT	NASA Scatterometer
OLS	Operational Line Scanner
PM	Passive Microwave
QUICKSCAT	NASA Quick Scatterometer
SMMR	Scanning Multichannel Microwave Radiometer
SPOT	Systeme Pour l'observation de la Terre
SSM/I	Special Sensor Microwave Imager
Team	NASA Team Algorithm for interpreting passive microwave data.

Acknowledgements

This work was partially completed while APW was a Fulbright scholar at NASA/Goddard Space Flight Center, Greenbelt, MD. Mr. Rob Gersten of SSAI is thanked for his programming support. Ice observers aboard the Antarctic

research voyages that contributed data for this study are thanked for their efforts. The comments of three anonymous referees helped to significantly improve the paper.

References

- Ackley, S. F., & Keliher, T. (1976). Antarctic sea ice dynamics and its possible climatic effects. *AIDJEX Bulletin*, 33, 53–76.
- Ackley, S. F., Wadhams, P., Comiso, J. C., & Worby, A. P. (2003). Decadal decrease of Antarctic sea ice extent inferred from whaling records revisited on the basis of historical and modern sea ice records. *Polar Research*, 22(1), 19–25.
- Allison, I., Brandt, R. E., & Warren, S. G. (1993). East Antarctic sea ice: albedo, thickness distribution, and snow cover. *Journal of Geophysical Research*, 98(C7), 12,417–12,429.
- Armand, L. K., & Leventer, A. (2003). Palaeo sea ice distribution—reconstruction and palaeoclimatic significance. In D. Thomas, & G. Dieckman (Eds.), *Sea ice—an introduction to its physics, biology, chemistry, and geology* (pp. 333–372). Oxford, UK: Blackwell Science.
- Bjørge, E., Johannessen, O. M., & Miles, M. W. (1997). Analysis of merged SSMR–SSMI time series of Arctic and Antarctic sea ice parameters 1978–1995. *Geophysical Research Letters*, 24(4), 413–416.
- Cavalieri, D. J., Gloersen, P., Parkinson, C. L., Comiso, J. C., & Zwally, H. J. (1997). Observed hemispheric asymmetry in global sea ice changes. *Science*, 278, 1104–1106.
- Comiso, J. C. (1995). SSM/I sea ice concentrations using the Bootstrap algorithm, *NASA Reference Publication* 1380, NASA/Goddard Space Flight Center, Greenbelt, MD, 49 pp.
- Comiso, J. C. (2003). Large scale characteristics and variability of the global sea ice cover. In D. Thomas, & G. Dieckman (Eds.), *Sea ice—an introduction to its physics, biology, chemistry, and geology* (pp. 112–142). Oxford, UK: Blackwell Science.
- Comiso, J. C., Cavalieri, D. J., Parkinson, C. L., & Gloersen, P. (1997). Passive microwave algorithms for sea ice concentration: A comparison of two techniques. *Remote Sensing of Environment*, 60, 357–384.
- Comiso, J. C., & Steffen, K. (2001). Studies of Antarctic sea ice concentrations from satellite data and their applications. *Journal of Geophysical Research*, 106 (C12), 31361–31385.
- Comiso, J. C., & Zwally, H. J. (1984). Concentration gradients and growth/decay characteristics of the seasonal sea ice cover. *Journal of Geophysical Research*, 89 (C5), 8081–8103.
- Crosta, X., Pichon, J.-J., & Burckle, L. H. (1998). Application of modern analog technique to marine Antarctic diatoms: Reconstruction of maximum sea-ice extent at the last glacial maximum. *Paleoceanography*, 13(3), 284–297.
- Curran, M. A., van Ommen, T. D., Morgan, V. I., Phillips, K. L., & Palmer, A. S. (2003). Ice core evidence for Antarctic sea ice decline since the 1950s. *Science*, 302, 1203–1206.
- de la Mare, W. K. (1997). Abrupt mid-twentieth-century decline in Antarctic sea-ice extent from whaling records. *Nature*, 389, 57–60.
- Gloersen, P., & Campbell, W. J. (1991). Recent variations in Arctic and Antarctic sea-ice covers. *Nature*, 352, 33–36.
- Gloersen, P., Campbell, W. J., Cavalieri, D. J., Comiso, J. C., Parkinson, C. L., & Zwally, H. J. (1992). *Arctic and Antarctic sea ice*. Washington, DC: NASA SP-511, NASA, 290 pp.
- Grenfell, T. C., Cavalieri, D. J., Comiso, J. C., Drinkwater, M. R., Onstott, R. G., Rubinstein, I., Steffen, K., & Winebrenner, D. P. (1992). Considerations for microwave remote sensing of thin sea ice. In F. D. Carsey (Ed.), *Microwave remote sensing of sea ice. Geophysical Monograph Series. Vol. 68* (pp. 291–301). Washington, DC: AGU.
- Jacobs, S. S., & Comiso, J. C. (1993). A recent sea-ice retreat west of the Antarctic Peninsula. *Geophysical Research Letters*, 20 (12), 1171–1174.
- Jones, D. A., & Simmonds, I. (1993). A climatology of southern hemisphere extratropical cyclones. *Climate Dynamics*, 9, 131–145.
- Kwok, R., Cunningham, G. F., & Yueh, S. (1999). Area balance of the Arctic ocean perennial ice zone: October 1996 to April 1997. *Journal of Geophysical Research*, 104 (C11), 25747–25759.
- Manabe, S., Spellman, M. J., & Stouffer, R. J. (1992). Transient responses of a coupled ocean–atmosphere model to gradual changes of atmospheric CO₂: Part II. Seasonal response. *Journal of Climate*, 5(2), 105–126.
- Massom, R. A., Drinkwater, M., & Haas, C. (1997). Winter snow cover on sea ice the Weddell sea. *Journal of Geophysical Research*, 102(C1), 1101–1117.
- Matzler, C., Ramsieir, R. O., & Svendsen, E. (1984). Polarization effects in sea ice signatures. *IEEE Journal of Oceanic Engineering*, OE-9, 333–338.
- Parkinson, C. L. (1990). Search for the little ice age in Southern ocean sea ice records. *Annals of Glaciology*, 14, 221–225.
- Parkinson, C. L., Cavalieri, D. J., Gloersen, P., Zwally, H. J., & Comiso, J. C. (1999). Arctic sea ice extents, areas, and trends, 1978–1996. *Journal of Geophysical Research*, 104(C9), 20837–20856.
- Schweitzer, P. N. (1995). *Monthly averaged polar sea ice concentration*. US Geological Survey Digital Data Series: Virginia, CD, Ed. 1. DDS-27.
- Stössel, A., Lemke, P., & Owens, W. B. (1990). Coupled sea ice–mixed layer simulations for the Southern ocean. *Journal of Geophysical Research*, 95(C6), 9539–9555.
- Sullivan, C. W., McClain, C., Comiso, J. C., & Smith Jr., W. O. (1988). Phytoplankton standing crops within an Antarctic ice edge. *Journal of Geophysical Research*, 93, 12487–12498.
- Wadhams, P., Lange, M. A., & Ackley, S. F. (1987). The ice thickness distribution across the Atlantic sector of the Antarctic ocean in midwinter. *Journal of Geophysical Research*, 92(C13), 14535–14552.
- Worby, A. P. (1999). *Observing Antarctic Sea Ice—A practical guide for conducting sea ice observations from vessels operating in the Antarctic pack ice*. CD-ROM, Scientific Committee on Antarctic Research (SCAR) Antarctic Sea Ice Processes and Climate (ASPeCt) program, Hobart, Tasmania, Australia.
- Worby, A. P., & Allison, I. (1999). A ship-based technique for observing Antarctic sea ice: Part I. Observational Techniques and Results, *Antarctic CRC Research Report* 14, 63 pp.
- Worby, A. P., Massom, R. A., Allison, I., Lytle, V. I., & Heil, P. (1998). East Antarctic sea ice: A review of its structure, properties and drift. In M. O. Jeffries (Ed.), *Antarctic sea ice physical processes, interactions and variability. Antarctic Research Series. Vol. 74* (pp. 41–67). Washington, DC: AGU.
- Wu, X., Budd, W. F., & Jacka, T. H. (1999). Simulations of Southern Hemisphere warming and Antarctic sea ice changes using global climate models. *Annals of Glaciology*, 29, 61–65.
- Zwally, H. J., Comiso, J. C., Parkinson, C., Cavalieri, D., & Gloersen, P. (2002). Variability of the Antarctic sea ice cover. *Journal of Geophysical Research*, 107(C5), 1029–1047.
- Zwally, H. J., Comiso, J. C., & Walsh, J. E. (1991). Variability of Antarctic sea ice. (abstract only). In Weller, G., C. L. Wilson, B. A. B. Severin (Eds.), *Proceedings of the International Conference on the Role of the Polar Regions in Global Change*. (p. 22). Fairbanks, Alaska: University of Alaska Fairbanks.